ISBN: 978-3-95450-211-0 doi:10.18429/JACoW-SRF2019-THP043

DEPOSITION PARAMETER EFFECTS ON NIOBIUM NITRIDE (NbN) THIN FILMS DEPOSITED ONTO COPPER SUBSTRATES WITH DC MAGNETRON SPUTTERING

S. Leith[1], M. Vogel[1], X. Jiang[1], E. Seiler[2], R, Ries[2]
[1]Institute of Materials Engineering, University of Siegen, Siegen, Germany
[2]Institute of Electrical Engineering SAS, Bratislava, Slovakia

Abstract

NbN thin films have been the subject of considerable research since the 1980's, firstly to be utilised in Josephson junctions or more recently, as part of multilayer coatings for superconducting radio frequency (SRF) cavities. So far their deposition has been limited to commercially available substrates such as Si and MgO, or Nb. As part of efforts to investigate their potential use with SRF cavities, results from a screening study probing the effects of various deposition parameters on the resulting film microstructure, phase formation and subsequent superconducting properties of NbN thin films deposited onto copper are presented. The substrate temperature, process pressure, bias voltage, Ar/N_2 ratio, gas type and cathode power were alternated between a high and low value. The resulting films were characterised using, among others, scanning electron microscopy (SEM), x-ray diffraction (XRD) and a DC magnetisation setup. Initial results indicate a large variance in the microstructure and superconducting properties with the change in deposition parameters.

INTRODUCTION

As part of efforts to improve the performance and reduce the costs of SRF cavities, alternative materials or procedures are currently being investigated to replace bulk niobium cavities. NbN is one of the alternative materials under investigation to provide these better performance figures. One of the most promising approaches is to use NbN in a multilayer superconductor-insulator-superconductor (SIS) coating, as first proposed by A. Gurevich [1]. This was initially proposed for deposition on a bulk niobium cavity.

NbN, with its higher T_c(17 K) and H_{c1}(200 Oe) in bulk form, has been touted as one of the front runners for implementation in SIS multilayer coatings [2]. One of the issues facing NbN however, is ensuring the formation of the desired phase during thin film deposition. NbN is known to form in a number of phases, three of which are superconducting, with deposited thin film T_c's ranging from 11.6 K for the hexagonal ϵ-phase [3], 12-15 K for the tetragonal γ-phase [4] and up to 16 K for the cubic δ-phase [5]. The creation of atomic level nitrogen deficiencies, which lead to the formation of the non-superconducting β-phase Nb_2N, is possible if the nitrogen flow rate is insufficient during film deposition [6]. The phases of NbN_x exist in different Nb:N ratios [7]: (1) β-NbN, x = 0.4 - 0.5, (2) γ-Nb_4N_3, x = 0.75 – 0.8, (3) δ-NbN, x = 0.88 – 0.98 and 1.015 – 1.062, (4) ϵ-NbN, x = 0.92 - 1. The most critical parameter, with regards to phase formation, seems to be the Ar/N_2 ratio. However, the optimum ratio changes with the substrate temperature [8], and with the process pressure [9].

The formation of normal conducting oxides, oxynitrides and voids, between NbN grains, is a known issue with NbN film performance and is thought to lead to the high resistivity [10] and early flux penetration found in NbN films.

The effects of deposition parameters on film growth and phase formation was investigated in order to realise an optimum parameter set for high performance films. The films were grown on copper substrates, in order to investigate their use as standalone thin film coatings, as well as on silicon substrates. The effects of the deposition parameters on the NbN film growth and the subsequent phase formation is discussed. This is the first known publication detailing the deposition of NbN onto copper for SRF applications.

EXPERIMENTAL

NbN thin films were deposited onto copper substrates and silicon witness samples via DC reactive magnetron sputtering using a Nb (RRR 300) target in a commercial high-volume, fully automated coating tool (CemeCon CC800) in the presence of a mixture of argon (99.998 Vol-%) or krypton (99.999 Vol-%) and nitrogen (99.999 Vol-%). The Ar or Kr to N_2 ratio was maintained via flow rate control of the two gases. The copper samples were initially mechanically polished and then chemically etched with nitric acid, which produced a surface roughness of R_q = 0.107 µm.

Prior to deposition, the system was passively baked at 650 °C for 6 hours, to assist in removing any built up adsorbents, and thereafter evacuated to a base pressure of 5 x 10^{-7} hPa. The system was then backfilled to a pressure of 1.5 x 10^{-3} hPa for target plasma cleaning and sputter etching of the copper substrate in an Ar atmosphere.

Following this, the chamber was set to the parameters required, depending on the sample in question. Samples were deposited for a screening study based on a Design of Experiments (DoE) approach, which utilised a high and low value for all parameters for both argon and krypton process gases. The values of the parameters are detailed in Table 1.

Table 1: NbN Film Deposition Parameter Set

Parameter boundary	Substrate Temp [°C]	Pressure [mPa]	Substrate Bias [V]	N_2 content [%]	Process Gas	Cathode Power [W]
high (+)	600	1600	-80	30	Ar	500
low (-)	200	800	0	10	Kr	300

ISBN: 978-3-95450-211-0 doi:10.18429/JACoW-SRF2019-THP043

Following the deposition of the films, samples were immediately placed in a Zeiss Ultra 55 Scanning Electron Microscope (SEM) to analyse the film microstructure. The silicon witness samples were cleaved in order to determine the thickness of each film and to explore the cross sectional structure of the film. The films were scanned with an EDX detector attached to the SEM, to determine contaminants like oxygen or carbon in the films, if any. The surface roughness of the samples was determined with both an Olympus LEXT OLS 4000 confocal laser scanning microscope (CLSM), with a scan size of 257 x 257 µm, and a Halcyonics XE-100 Atomic Force Microscope (AFM) in non-contact mode, with a scan size of 5 x 5 µm, to better understand the surface roughness at different length scales.

X-ray diffraction (XRD) θ - 2θ studies were completed on all samples, using a Panalytical Empyrean diffractometer with a Cu $K\alpha$ source, to assist with phase identification. X-ray photoelectron spectroscopy (XPS), using an Evans Analytical Group LLC XPS SSX-100, was used. The XPS setup used in this study is not fitted with a sputter device and was unable to sputter away the surface layer of the film. As such, the data provided information relating to the outermost ~10nm of the film.

Rutherford Backscattering Spectroscopy (RBS) was also conducted on five pre-screening test samples which were deposited at N_2/Ar flow concentrations of 10, 15, 20, 25 and 30%, with a high temperature, mid cathode power, high pressure and no bias in comparison to the screening test samples. RBS measurements were performed using a hydrogen beam with 0° angle of incidence, 165° scattering angle and 25° exit angle.

Sections of these same samples were sent to IEE in Bratislava for DC magnetisation studies to investigate the basic superconducting properties. Small samples of approximately 2x2 mm^2 were tested using Vibrating Sample Magnetometer (VSM) from Quantum Design Inc. In the experiments, a DC magnetic field of 5 mT was applied perpendicular to the flat face of the sample and the temperature T was subsequently decreased through the transition range at a rate of approximately 0.2 K/min. The magnetic moment m of the sample was measured at 0.1 K steps and the superconducting transition temperature T_c was taken as the onset of magnetic moment change. The variation in the baseline magnetic moment of the different samples is mostly due to volume effects of the different samples.

RESULTS AND DISCUSSION

All results detailed here are based on investigations of the NbN films deposited onto copper, except the SEM cross section images, which required the use of cleaved silicon samples. The cleaved Si samples provided an indication of the film thickness, with all films lying within the region of 1.2 ± 0.2 µm. The different deposition conditions resulted in deposition rates ranging from 11.4 to 49.5 nm/min, mostly affected by the Ar/N_2 ratio and the cathode power. Due to the parameters used in the sputter etching of the substrates, a thin interlayer (40 – 60 nm) of Nb was deposited on nearly all samples.

Figure 1: Optical image of hexagonal silver NbN film (left) and cubic gold NbN film (right).

Initial optical inspections of the samples showed films with either a silver or gold colour, as shown in Fig. 1. Generally the gold colour is said to indicate a cubic film structure (δ-NbN) while the silver colour indicates a hexagonal structure (β, ϵ or γ'-NbN) [11], however, this is not conclusive in itself, as in some instances, films which are gold in colour, display low T_c values and films with a silver colour display high T_c values. The films were found to have a dull finish, indicative of a fairly rough surface. This was supported by AFM, CLSM and SEM investigations, where the surface was found to closely conform to the underlying copper surface as evidenced in Fig. 2.

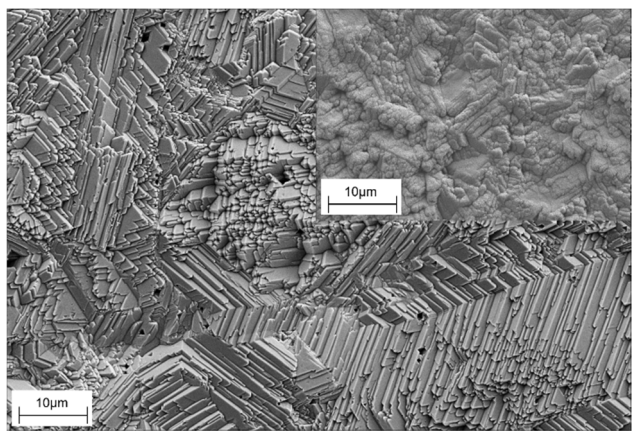

Figure 2: SEM images of Cu substrate following: (Main) Nitric acid etching and (Inset) NbN thin film coated Cu sample detailing close matching of film to substrate morphology.

The surface roughness measurements, conducted using both the AFM and CLSM, provided topographical information at two different length scales. The deposition parameter effects on the surface roughness are detailed in Table 2, with (+) indicating an increase in surface roughness and (-) indicating a decrease in surface roughness.

Both the AFM and CLSM measurements detail similar trends in terms of the deposition parameter influence on the surface roughness. All parameters except the substrate temperature were found to influence the resultant surface. The AFM measurements displayed greater variability in surface roughness between the high and low deposition parameters, indicating a more noticeable influence at smaller length scales, indicating a large effect on film microstructure, such as grain morphology.

ISBN: 978-3-95450-211-0 doi:10.18429/JACoW-SRF2019-THP043

The biggest influence is found to be due to the change from Ar to Kr gas. Which results in a 30 – 40 % reduction in surface roughness.

Table 2: Deposition Parameter Effect on Surface Roughness

Parameter boundary	Substrate Temp [°C]	Pressure [mPa]	Substrate Bias [V]	N_2 content [%]	Process Gas	Cathode Power [W]
High	Equal	-	+	-	+	+
Low	Equal	+	-	+	-	-

Generally, NbN films are said to grow in a columnar fashion [12]. Based on SEM investigations completed in this study, growth modes within NbN films are found to vary significantly depending on the deposition conditions.

For a dense film, a high substrate temperature is preferred, but not mandatory, provided that a substrate bias and high cathode power is applied, as shown in Fig. 3.

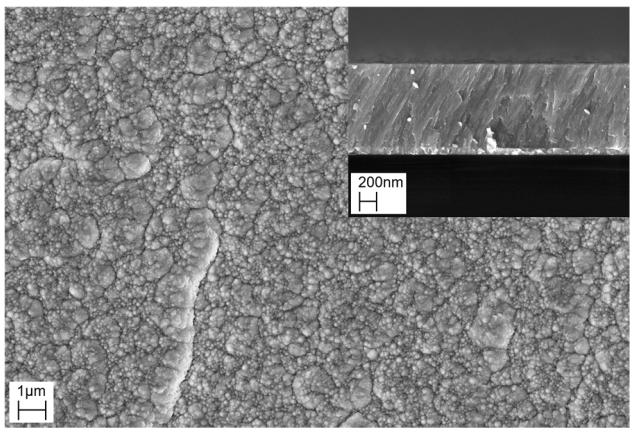

Figure 3: SEM images detailing low substrate temperature effects overcome by use of bias and high cathode power to produce dense film. (Main) Plain view of film on Cu. (Inset) Cross section view of film on Si.

The process pressure is found to have a large impact on the growth mechanism, with high pressure tending to grow porous and highly disconnected columnar films, while low pressure deposition leads to dense films and adherent columns, as detailed in Fig. 4.

A high cathode power in nearly all cases is needed for a dense film however, an applied substrate bias can compensate for a lack of power, provided that there is a high enough mean-free-path (low pressure). The substitution of Ar with Kr as working gas, and the variation in N_2 % does not seem to change the growth modes significantly within this parameter window.

The results from EDX scans of the NbN films provided details regarding the oxygen content of the coatings. Samples deposited using Kr gas were found to repeatedly contain more oxygen than their Ar counterparts, while Lower process pressure leads to a decreased level of oxygen within the films. This is currently under investigation.

The RBS analysis, completed on the pre-screening samples, indicated a changing Nb:N ratio in the deposited thin films when different N_2 concentrations were used during deposition. The results are detailed in Table 3.

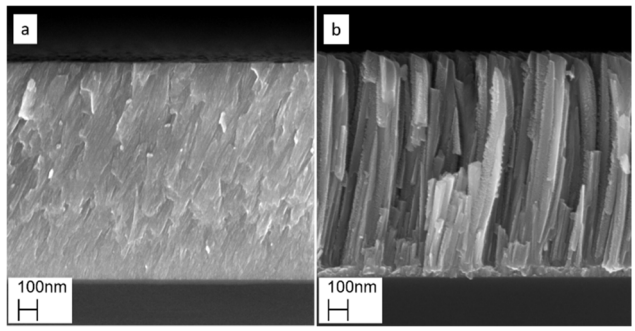

Figure 4: SEM images showing (a) Low pressure films grow dense and adherent structure. (b) Same deposition parameters with a high pressure produce porous columnar growth

Table 3: Elemental Composition of NbN Thin Films Deposited with Differing N2 Flow Rates

N_2 flow %	Nb (at.%)	N (at.%)	O (at.%)	x
10	48.8	46.2	5	0.95
15	48.75	45.17	6.07	0.93
20	48.30	45.75	6	0.95
25	45.71	51.37	2.90	1.12
30	48.70	50.86	0.43	1.04

Films coated with ≤ 20 % N flow rate are found to be under stoichiometric and within the range defined by Oya [7] for δ-NbN while those deposited with > 20 % are over stoichiometric, however the 30 % N2 film is still within the δ-NbN band defined by Oya.

The high percentage of N within the films indicates a lack of the β-NbN and γ-NbN phases, x = 0.4 to 0.8, for these deposition parameters. The decrease in oxygen content in the films with increasing nitrogen flow, also confirmed with EDX analysis, will affect the absolute stoichiometry of the NbN films. The presence of oxygen can be linked to the higher base pressure of the system used, the use of 4.8 purity argon and the formation of the native oxide layer since removal from the sputtering chamber. The increase in nitrogen flow rate is understood to decrease the likelihood of oxygen inclusion due to a decreased ratio of oxygen to nitrogen in the deposition chamber.

The XPS data of all measured samples were very similar, indicating no significant difference due to the deposition conditions. Figure 5 shows the Nb3d and N1s spectrums and their deconvolution for an indicative sample scan.

The data indicates the presence of a Nb_2O_5 oxide layer indicated by the ~207 eV peak in the Nb3d spectrum [13]. A series of oxynitrides (NbO_xN_{1-x}) which are known to decrease the superconducting performance of NbN thin films, are indicated by the ~400 eV and ~401.4 eV peak in the N1s spectrum [13]. NbN is detailed in both the N1s spectrum (~397 eV) and the Nb3d spectrum (~204eV) [14]. The oxynitrides are said to disappear following the removal of the surface oxide layer [14,15], which was not done in this study as mentioned earlier. No unbound Nb, characterised by a peak at ~202.4 eV in the Nb3d spectrum, was found, providing evidence for the lack of the β-phase in XRD scans.

ISBN: 978-3-95450-211-0 doi:10.18429/JACoW-SRF2019-THP043

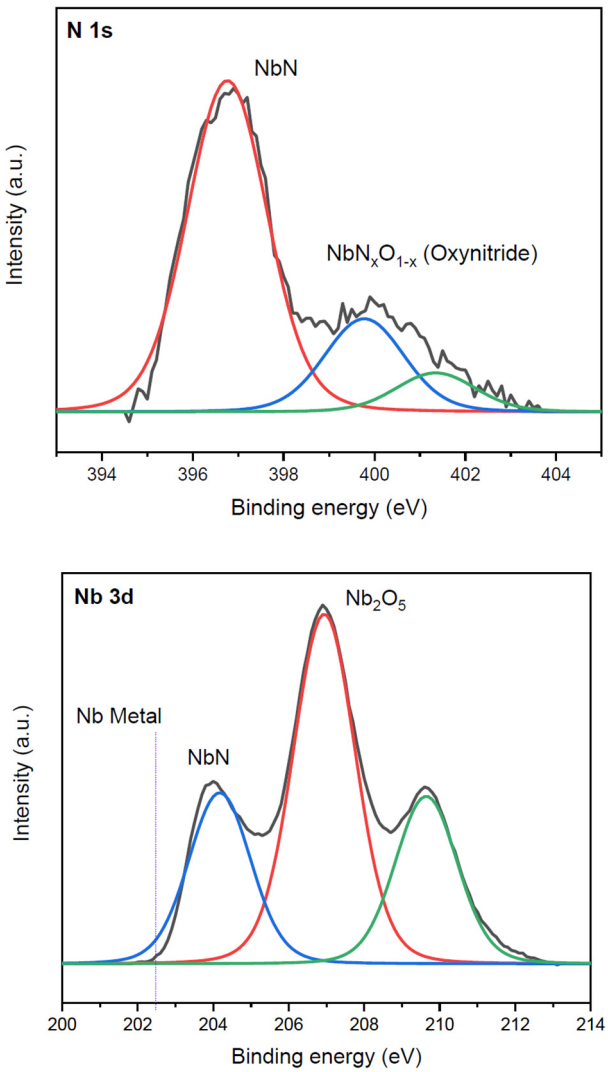

Figure 5: XPS indicative scans of the outer 10nm of NbN film surface. N1s (Top) and Nb3d (Bottom) In general, all films exhibit similar profiles.

XRD (θ-2θ) scans were performed on all NbN/Cu samples and produced varying profiles for the different deposition conditions, with a subset of representative scans presented in Fig. 6. Due to the nature of the overlapping NbN peaks, it is known to be challenging to characterise NbN phases from XRD data alone [16]. The figure shows three selected samples which correspond to the T_c measurements described below. Sample (a) features a phase mixture of δ and ε-NbN. Here the Nb interlayer can be detected and shows to be aligned along a growth direction of [110], evident through the (110) and corresponding (220) XRD peaks. Sample (b) and (c) are identified as cubic δ-NbN films. While (b) shows relatively sharp NbN peaks which are oriented along the [111] growth direction, the NbN peaks in (c) are broadened and exhibit a different growth orientation in [100] direction. The SEM cross sections of sample (b) and (c), not shown here, are in good consistency to the XRD results. Sample (b) feature a columnar growth with a diameter of more than 100 nm, explaining the found

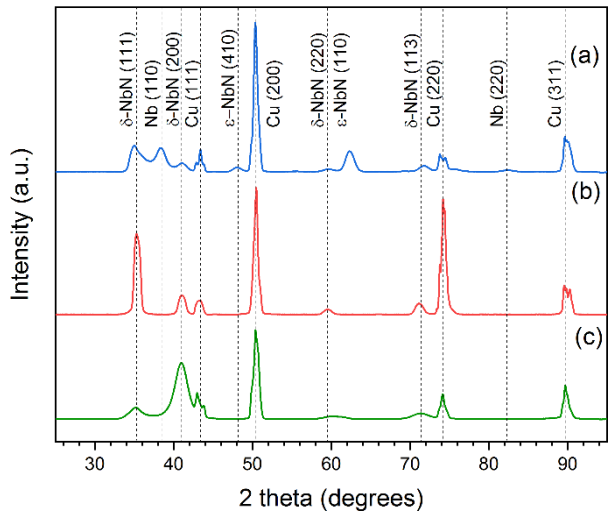

Figure 6: XRD scans of three NbN thin film samples indicating the general results of all films.

orientation and sharp peaks, while for (c) the columns are a few nm in diameter which, in turn, leads to broadened XRD peaks.

The T_c results for the same selection of samples as described above in the XRD section are presented in Fig. 7. All the investigated samples were found to be superconducting, with T_c ranging from 8.2 K to 14.8 K, with the larger Ar/N_2 ratio films proving to be superior. Sample (a) presents two distinct transition points at 8.2 K and 10.8 K, which indicates the presence of two separate superconducting phases, as confirmed by the XRD analysis. Sample (b) shows the highest T_c which is in compliance with the above discussed XRD and SEM results. Crystal size and/or orientation seems to lead to a decrease in the T_c, as revealed by sample (c).

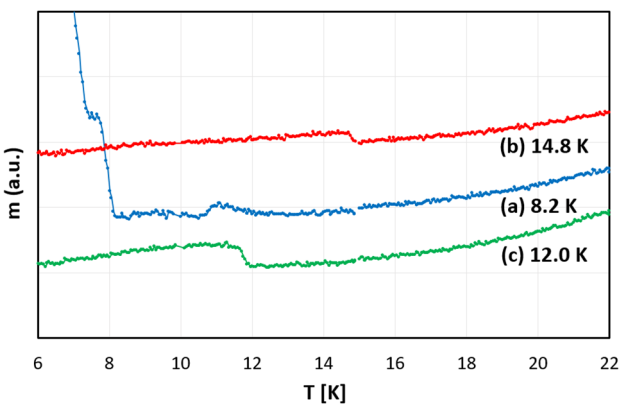

Figure 7: m(T) measurements of NbN thin film samples. The determined T_c values are stated.

CONCLUSION

It has been shown that the synthesis of a superconducting NbN phase is possible on a polycrystalline Cu substrate. Further studies will exploit NbN's potential in a multi-layered coating system on Cu substrates. A first set of conclusions are given: in an attempt to avoid the possible formation of voids and/or oxynitride inclusions in between

ISBN: 978-3-95450-211-0 doi:10.18429/JACoW-SRF2019-THP043

NbN grains, dense films with adherent columns should be pursued. Thus a high substrate temperature and a low process pressure are recommended as well as a relatively high cathode power, keeping in mind the requirement for sufficient nitrogen to react with niobium.

One critical parameter for the formation of the δ – NbN phase is the use of lower nitrogen flows (10 %).

The use of Kr instead of Ar as a working gas leads to a lower surface roughness at smaller length scales. A lower nitrogen flow rate during deposition results in superior superconducting properties, however it leads to an increased oxygen content compared to higher nitrogen flow rates.

ACKNOWLEDGEMENTS

This work forms part of the EASITrain Marie Sklodowska-Curie Action (MSCA) Innovative Training Networks (ITN) which has received funding from the European Union's H2020 Framework Programme under Grant Agreement no. 764879.

Part of this work was performed at the Micro- and Nanoanalytics Facility (MNaF) of the University of Siegen.

The DC magnetisation measurements and RBS analysis were completed under the European Union's ARIES collaboration H2020 Research and Innovation Programme under Grant Agreement no. 730871

REFERENCES

[1] A. Gurevich, "Enhancement of rf breakdown field of superconductors by multilayer coating," *Appl. Phys. Lett.*, vol. 88, no. 1, p. 012511, Jan. 2006.

[2] M. R. Beebe, D. B. Beringer, M. C. Burton, K. Yang, and R. A. Lukaszew, "Stoichiometry and thickness dependence of superconducting properties of niobium nitride thin films," *J. Vac. Sci. Technol. A Vacuum, Surfaces, Film.*, vol. 34, no. 2, p. 021510, Mar. 2016.

[3] Y. Zou *et al.*, "Discovery of Superconductivity in Hard Hexagonal ε-NbN," *Sci. Rep.*, vol. 6, no. 1, p. 22330, Apr. 2016.

[4] G. V. Eremeev, "Review of RF Properties of NbN and MgB2 Thin Coating on Nb Samples and Cavities", in *Proc. 14th Int. Conf. RF Superconductivity (SRF'09)*, Berlin, Germany, Sep. 2009, paper TUOBAU08, pp. 159-163.

[5] S. P. Chockalingam, M. Chand, J. Jesudasan, V. Tripathi, and P. Raychaudhuri, "Superconducting properties and Hall effect of epitaxial NbN thin films," *Phys. Rev. B - Condens. Matter Mater. Phys.*, vol. 77, no. 21, p. 214503, Jun. 2008.

[6] D. Hazra *et al.*, "Superconducting properties of very high quality NbN thin films grown by high temperature chemical vapor deposition," *Supercond. Sci. Technol.*, vol. 29, no. 10, p. 105011, Oct. 2016.

[7] G. Oya and Y. Onodera, "Transition temperatures and crystal structures of single-crystal and polycrystalline NbN x films," *J. Appl. Phys.*, vol. 45, no. 3, pp. 1389–1397, Mar. 1974.

[8] Y. M. Shy, L. E. Toth, and R. Somasundaram, "Superconducting properties, electrical resistivities, and structure of NbN thin films," *J. Appl. Phys.*, vol. 44, no. 12, pp. 5539–5545, 1973.

[9] J. C. Villegier, L. Vieux-Rochaz, M. Goniche, P. Renard, and M. Vabre, "NbN Tunnel Junctions," *IEEE Trans. Magn.*, vol. 21, no. 2, pp. 498–504, 1985.

[10] S. Isagawa, "rf superconducting properties of reactively sputtered NbN," *J. Appl. Phys.*, vol. 52, no. 2, pp. 921–927, Feb. 1981.

[11] F. Mercier *et al.*, "Niobium nitride thin films deposited by high temperature chemical vapor deposition," *Surf. Coatings Technol.*, vol. 260, pp. 126–132, 2014.

[12] S. Wilde et al., "Physical Vapour Deposition of NbTiN Thin Films for Superconducting RF Cavities", in *Proc. 8th Int. Particle Accelerator Conf. (IPAC'17)*, Copenhagen, Denmark, May 2017, pp. 1102-1104. doi:10.18429/JACoW-IPAC2017-MOPVA104

[13] G. Jouve, C. Séverac, and S. Cantacuzène, "XPS study of NbN and (NbTi)N superconducting coatings," *Thin Solid Films*, vol. 287, no. 1–2, pp. 146–153, Oct. 1996.

[14] K. S. Havey, J. S. Zabinski, and S. D. Walck, "The chemistry, structure, and resulting wear properties of magnetron-sputtered NbN thin films," *Thin Solid Films*, vol. 303, no. 1–2, pp. 238–245, Jul. 1997.

[15] J. Halbritter and A. Darlinski, "Angle resolved XPS studies of oxides at NbB, NbC, and Nb surfaces," *Surf. Interface Anal.*, vol. 10, no. May 1986, pp. 223–237, 1987.

[16] M. Benkahoul, E. Martinez, A. Karimi, R. Sanjinés, and F. Lévy, "Structural and mechanical properties of sputtered cubic and hexagonal NbNxthin films," *Surf. Coatings Technol.*, vol. 180–181, pp. 178–183, 2004.